Brazilian Dental Science

unesp
UNIVERSIDADE ESTADUAL PAULISTA
"JÚLIO DE MESQUITA FILHO"
Instituto de Ciência e Tecnologia
Campus de São José dos Campos

Original Article

DOI: https://doi.org/10.4322/bds.2026.e5261

Influence of a new light-curing system with optical fiber on the cementation of 3D-printed intraradicular posts

Influência de um novo sistema de fotopolimerização com fibra óptica na cimentação de pinos intrarradiculares impressos em 3D

Mariana Fernanda SOUZA[1], **Juliana de Freitas Gouveia SILVA**[1], **Carolina Gonzales FRANÇA**[1], **Lais Carolina Landim GOMES**[2], **Tarcisio José de Arruda PAES JUNIOR**[1]

1 - Universidade Estadual de São Paulo, Instituto de Ciência e Tecnologia, Departamento de Materiais Dentários e Prótese Dentária. São José dos Campos, SP, Brazil.
2 - University of Saskatchewan, College of Dentistry. Saskatoon, Saskatchewan, Canada.

How to cite: Souza MF, Silva JFG, França CG, Gomes LCL, Paes Junior TJA. Influence of a new light-curing system with optical fiber on the cementation of 3D-printed intraradicular posts. Braz. Dent. Sci. 2026;29: e5261. https://doi.org/10.4322/bds.2026.e5261

ABSTRACT

Objective: To evaluate the bond strength between root dentin and composite resin associated with a 3D-printed intraradicular post customized with flowable resin, using a fiber optic light-curing system that photoactivates the resin from within the post. **Material and Methods:** Thirty bovine teeth were used and divided into three groups (n=10): PHOTO (P) conventionally light-cured post (control); FIBER (F) post light-cured with optical fiber; FIBER+PHOTO (F+P) post light-cured with both optical fiber and conventional curing. The internal channel of the printed post allowed insertion of the optical fiber along the entire post length, enabling light transmission throughout the root canal. Bond strength was assessed using the push-out test, in which a load of 50 kgf was applied at a crosshead speed of 0.5 mm/min using a universal testing machine (EMIC, São José dos Campos, Brazil) for the cervical, middle, and apical thirds. Data were analyzed using two-way ANOVA and Tukey's post hoc test (α=0.05). **Results:** There was a statistically significant difference between the root thirds, with higher bond strength values in the cervical third (4.224 ± 1.53 MPa), followed by the middle third (3.475 ± 1.32 MPa), and lower values in the apical third (1.768 ± 1.25 MPa). Furthermore, differences were observed in the distribution of failure types between the groups and the thirds evaluated. **Conclusion:** The root third significantly influenced bond strength, with higher values in the cervical region and lower values in the apical region. The light-curing system did not significantly affect bond strength; however, differences in failure patterns were observed among groups.

KEYWORDS

Dental curing lights; Intraradicular; Photopolymerization; Pins; Printed.

RESUMO

Objetivo: Avaliar a resistência adesiva entre a dentina radicular, e um compósito associado a um pino intrarradicular impresso, personalizado com resina fluida e, por emprego de um sistema de fibra óptica que fotoativa a resina a partir do interior do pino. **Material e Métodos:** Foram utilizados 30 dentes bovinos distribuídos em 3 grupos (n=10): Foto (F) - pino impresso fotopolimerizado de maneira convencional (controle); Fibra (F) - pino impresso fotopolimerizado com uso de fibra óptica; Fibra+Foto (F+F) - pino impresso fotopolimerizado de maneira convencional e com fibra óptica. O conduto interno do pino impresso permitiu a inserção da fibra óptica por toda a extensão do pino que permitisse a ação da luz ao longo do conduto radicular. Para a análise de resistência adesiva foi utilizada a técnica push out, em que foi aplicada uma carga de 50 kgf na velocidade de 0,5mm/min em uma máquina de ensaio universal (EMIC, São José dos Campos) para os terços cervical, médio e apical. Os dados computados foram submetidos à análise estatística ANOVA dois-fatores e teste de Tukey. **Resultados:** Houve diferença estatisticamente significativa entre os terços radiculares, com maiores valores de resistência de união no terço cervical (4,224 ± 1,53 MPa), seguidos pelo terço médio (3,475 ± 1,32 MPa) e menores

This is an Open Access article distributed under the terms of the Creative Commons Attribution license (https://creativecommons.org/licenses/by/4.0/), which permits unrestricted use, distribution, and reproduction in any medium, provided the original work is properly cited.

valores no terço apical (1,768 ± 1,25 MPa). Além disso, foram observadas diferenças na distribuição dos tipos de falhas entre os grupos e os terços avaliados. **Conclusão:** O terço radicular influenciou significativamente a resistência de união, com valores mais altos na região cervical e mais baixos na região apical. O sistema de fotopolimerização não afetou significativamente a resistência de união; no entanto, diferenças nos padrões de falha foram observadas entre os grupos.

PALAVRAS-CHAVE

Luz de cura dentária; Intrarradicular; Fotopolimerização; Pinos; Impresso.

INTRODUCTION

Restorations of endodontically treated teeth with extensive coronal loss due to large carious lesions or dental fractures often require intraradicular posts as a critical component of the retention system for the coronal restoration. Among the available treatment options, glass fiber posts are the most widely used due to their favorable esthetic properties, ease of handling, and elastic modulus similar to that of dentin [1-4]. However, despite these advantages, prefabricated posts present certain limitations, including suboptimal canal adaptation and a predominance of adhesive failures at the post-dentin interface [5-7].

In addition to the selection of an appropriate post, the success of endodontic restorations is directly related to the choice of the adhesive system and resin cement used during the luting procedure. Consequently, adequate polymerization of these materials within the apical portion of the root canal must be ensured. Although translucent fiber posts allow light transmission, light attenuation along the root canal remains a clinically relevant challenge and has been associated with a reduction in degree of conversion and bond strength in the apical region, as demonstrated in the literature [8,9]. Therefore, the use of dual-cure or chemically activated adhesive systems is frequently recommended to overcome this limitation [10,11].

However, even though dual-cure and self-cure resin cement were specifically developed for post cementation, studies have demonstrated that in the absence of adequate light activation, some dual-cure cements fail to achieve a sufficient degree of conversion, which may range from 35% to 80%, resulting in inefficient polymerization [12-15]. Despite this, there is still no consensus in the literature regarding clinical strategies capable of ensuring adequate polymerization in deeper regions of the root canal, as light transmission along the canal decreases progressively with depth and is directly associated with a reduction in the degree of conversion in the apical region [8,16,17]. Consequently, given the dependence on light for optimal polymerization, the apical portion of root canals may exhibit compromised adhesion due to a higher concentration of unreacted monomers retained in the cement layer [8,16]. This incomplete polymerization can lead to adverse outcomes, including adhesive failure, reduced wear resistance, microleakage, inflammatory tissue reactions, increased water sorption and solubility, and color instability [18-22].

In this context, three-dimensional (3D) printing technology offers new possibilities for dental treatments by enabling the fabrication of objects with customized size and geometry through a layer-by-layer construction process, thereby allowing high precision in restoration manufacturing [23,24]. The characteristics of 3D-printed objects vary depending on several factors, including the nature of the material used (plastics, ceramics, metals or resins), the deposition technology employed, the layer formation mechanism, and the material composition. These variables collectively influence critical outcomes such as surface finish, texture, geometric accuracy, and mechanical properties [2].

Therefore, in pursuit of novel photopolymerization methods that are both accessible and effective throughout the entire root canal extension, combined with innovative fabrication techniques such as 3D printing, this study aimed to evaluate the bond strength between root dentin and composite resin used to cement 3D-printed custom perforated intraradicular posts personalized with flowable composite resin. A novel fiber optic light-curing system capable of photoactivation along the entire canal length was employed, and adhesive failure patterns across different root thirds were compared among the experimental groups.

MATERIALS AND METHODS

Fabrication of posts

The perforated printed posts were designed using Rhinoceros 5.0 software (Seattle, USA), measuring 16 mm in length and 1.6 mm in regular diameter to allow passage of the optical fiber. The hollow internal extension permitted the insertion of an optical fiber along the entire length of the post to direct the light action throughout the root canal, especially in the apical portion. The thickness of the wall post was 0.4 mm (from the cervical to apical portion) (Figure 1).

The design was exported in STL format to the printer slicing software, programmed for printing with a 100 μm layer thickness, using Bio Splint resin (Prizma, MakertechLabs), in a transparent color to allow light transmission through the post for resin and cement polymerization. Printing was performed on an Anycubic Photon Mono SE printer (Shenzhen Anycubic Technology Co., Ltd., Shenzhen, China). After printing, the samples underwent the manufacturer's recommended cleaning protocol, being immersed in isopropyl alcohol for 5 minutes, followed by post-curing (polymerization) using the Anycubic Photon Mono SE photopolymerizer (wavelength of 405 nm) for 15 minutes to ensure complete polymerization and achieve ideal mechanical properties of the resin.

Sample preparation

Thirty intact bovine single-rooted teeth (incisors) with a single root canal and no apical curvature were selected for sample preparation. The teeth were cleaned, stored in saline solution, and frozen until use. The crown of each tooth was sectioned at the cementoenamel junction

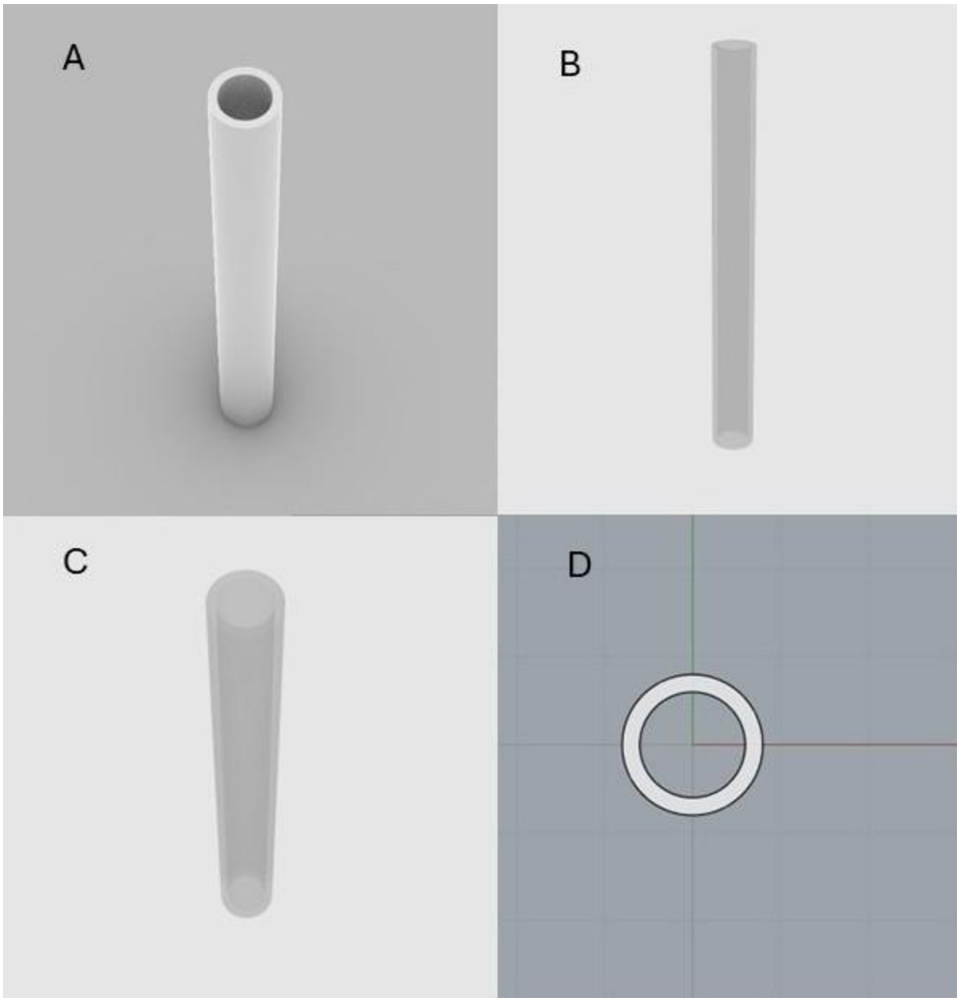


Figure 1 - Schematic representation of the custom-made hollow 3D-printed intraradicular post designed using Rhinoceros 5.0 software. **Legend: (A)** Three-dimensional perspective view of the post. **(B)** Lateral view showing the standardized dimensions (16 mm in length and 1.6 mm in external diameter). **(C)** Semi-transparent view illustrating the central lumen extending throughout the post, designed to accommodate an optical fiber for light transmission along the root canal. **(D)** Cross-sectional view showing the 0.4-mm wall thickness and the central lumen intended to accommodate the optical fiber, allowing light transmission throughout the root canal.

using a diamond disc (KG Sorensen, Barueri, SP, Brazil) under refrigeration cooling, and only the roots were used for the experimental procedures. Conventional endodontic treatment was performed using a reciprocating system with R #40 files (Reciproc® – VDW, Germany), followed by irrigation with 2.5% sodium hypochlorite (Asfer Chemical Industry Ltd., SP, Brazil) and obturation with gutta-percha cones (Dentsply, SP, Brazil) and AH Plus Jet sealer (Dentsply Sirona, Brazil). Subsequently, approximately two-thirds of the root canal filling material was removed using Largo drills (Maillefer – Dentsply) to prepare the post space, following the conventional fiber post cementation protocol.

The roots were randomly assigned to experimental groups (n=10), according to the different photopolymerization methods used, as shown in Table 1.

Activation system with fiber optic light guide

Optical fibers are widely recognized as dielectric waveguides consisting of a cylindrical core surrounded by a cladding layer with a lower refractive index. Light propagates through the optical fiber primarily via the principle of total internal reflection.

In the present study, a custom metal coupling device with a small aperture was developed to accommodate a 1 mm diameter circular-section optical fiber cable. Through this device, LED light emitted by a Radii-cal photopolymerizer (SDI Limited, Victoria, Australia) with an irradiance of 1200 mW/cm^2 was conducted along the entire root canal length to the apical region, thereby enabling more effective activation of the resin cement throughout the canal extension.

The accessory light-delivery device received patent approval from the Brazilian National Institute of Industrial Property (INPI) in 2020 (Patent No. BR 10 2020 025592 4) (Figure 2).

Calculation of the photoactivation time for the new photopolymerization system

To determine the appropriate photoactivation time for the novel photopolymerization system, the time required for the resin cement in each root canal third to achieve a radiant exposure of 16 J/cm^2 was calculated. For this purpose, a laser power meter (Nova Handheld Laser Power Meter, Ophir Optronics, Jerusalem, Israel) was used to measure the optical power output of the Radii-cal LED device (SDI Limited, Victoria, Australia) coupled with the fiber optic system, which yielded a value of 1.626 mW.

To calculate the irradiance, the cross-sectional area of the optical fiber tip (0.00785 cm^2) was considered, resulting in an irradiance of 207.13 mW/cm^2 (equivalent to 0.207 J/s·cm^2). Finding a photoactivation time of 80 seconds. The photoactivation time was then calculated using the following Equation 1:

$$\text{Radiant exposure } (\text{J/cm}^2) = \text{Irradiance } (\text{W/cm}^2) \times \text{Time } (\text{s}) \quad (1)$$

where, Radiation Exposure = 16 (J) and Irradiance = 0.207 $\left(\frac{J}{cm^2}\right)$.

Customization of the printed posts

The printed posts were customized using Tetric N-Ceram A2 composite resin according to the anatomy of each root canal. For this purpose, petrolatum was applied inside the root canal, and the customization was performed by applying the composite resin directly onto the printed post. Finally, the customized post was removed from the canal and light-cured for 40 seconds

Table 1 – Distribution of groups according to the photopolymerization system and respective polymerization times

Groups (n=10)	Characteristics	Photoactivation time
PHOTO (control)	Perforated printed post, conventional light cured.	1 x 45-second activation (cervical third)
FIBER (F)	Perforated printed post, photopolymerized through optical fiber.	3 activations: 80 seconds (cervical third) + 80 seconds (middle third) + 80 seconds (apical third).
FIBER+PHOTO (F+P)	Perforated printed post, photopolymerized through optical fiber and conventional photopolymerization.	4 activations: 80 seconds (cervical third) + 80 seconds (middle third) + 80 seconds (apical third) + 45 seconds (cervical third - conventional way)

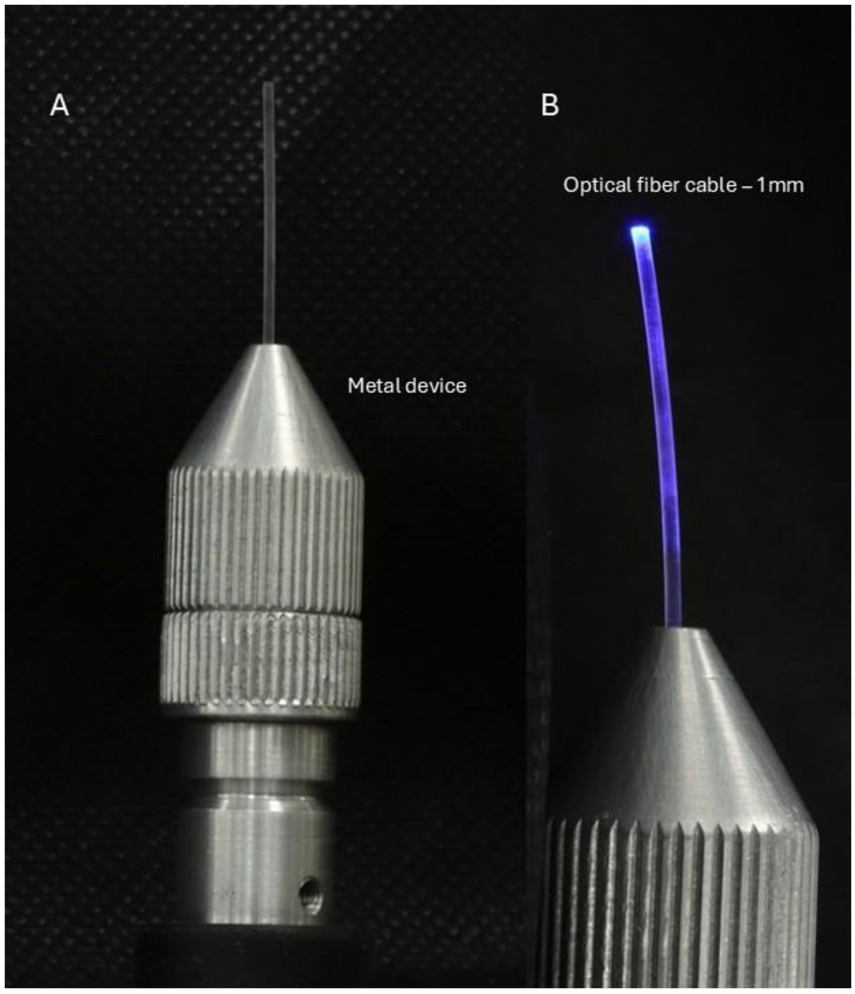


Figure 2 - Accessory photopolymerization device. **A)** Complete accessory photopolymerization device; **B)** Accessory device in operation coupled to the photopolymerizer.

Cementation of the posts

Root canals were prepared for post insertion using Largo burs #2 and #3 from the Exacto system (Angelus, Londrina, Brazil) to a depth of 16 mm, leaving 4 mm of gutta-percha in the apical region. Following preparation, canals were irrigated with 3 mL of 17% EDTA solution (Biodinâmica, Ibiporã, Brazil) for 3 minutes, followed by saline irrigation and drying with absorbent paper points (Tanari, Manacapuru, Brazil).

Post cementation was performed according to the manufacturer's instructions for Allcem Dual resin cement (FGM, Joinville, Santa Catarina, Brazil). Posts were cleaned in an ultrasonic bath with isopropyl alcohol, air-dried, and silanized using a silane coupling agent (Angelus, Londrina, Brazil).

For root canal conditioning, 37% phosphoric acid gel (Condac 37, FGM Dental Group, Joinville, Brazil) was applied for 15 seconds, followed by thorough rinsing with distilled water. Canals were then dried with absorbent paper points (Dentsply Sirona, São Paulo, Brazil), and Ambar adhesive system (FGM, Joinville, Santa Catarina, Brazil) was actively applied using a microbrush applicator (KG Sorensen, Cotia, Brazil). The resin cement was delivered into the root canal using an applicator syringe, the post was inserted, and excess cement was removed with a cotton pellet.

For groups receiving conventional indirect photoactivation (PHOTO), light curing was performed for 45 seconds at the cervical opening of each specimen. For the FIBER and FIBER+PHOTO groups, the LED device was coupled to the fiber optic accessory and inserted into the root canal until reaching the apical third. Photoactivation was performed at maximum power output for 80 seconds at this position. Subsequently, the fiber optic tip was retracted approximately 4 mm to photoactivate the middle third for 80 seconds, then retracted an additional 4 mm to photoactivate the cervical

third for 80 seconds. Each retraction distance was standardized using a positioning jig to ensure consistent measurements across all root thirds.

Sectioning of slices for mechanical testing

Following cement polymerization, specimens were mounted on a metal base in a precision cutting machine (Isomet 1000, Buehler, Lake Bluff, IL, USA) and sectioned perpendicular to the root's long axis using a diamond-coated disc (WFR BLDE 4" × 0.12" × 1/2", Extec, Enfield, CT, USA) under continuous water irrigation. For each specimen, slices approximately 2 mm thickness were obtained from the cervical, middle, and apical thirds for subsequent push-out testing. Specimens were stored in a light-proof container at room temperature until testing.

Push-out test

Slices with 2 mm thickness were obtained from the cervical, middle, and apical thirds (n=10). The samples were positioned on a metal device with a central opening larger than the canal diameter. The coronal surface of the specimen was placed downward, meaning the load was applied from the apical to the coronal direction until the post was displaced or the specimen fractured.

A metallic cylinder adapted to have a tip diameter of 1 mm applied the load to the center of the post without contacting the dentin. Since the specimens were sectioned perpendicular to their long axis, the load was applied parallel to the root axis.

The test was performed on a universal testing machine (EMIC DL-1000, Equipamentos e Sistemas Ltda, São José dos Pinhais, Brazil) at a speed of 0.5 mm/min and a 50 Kgf load cell.

Bond strength

Bond strength (σ) was calculated using the formula $\sigma = F/A$, where F represents the load at failure (N), and A represents the bonded interfacial area (mm^2). The bonded area (A) for each specimen was calculated using the formula for the lateral surface area of a frustum of a right circular cone (Equation 2):

$$A = \pi.g.(R1+R2) \quad (2)$$

where A = bonded interfacial area (mm^2), $\varpi = 3.14$, g = slant height of the frustum (mm), R_1 = post radius at the apical end (mm), R_2 = post radius at the cervical end (mm), and h = slice thickness (mm). The slant height (g) was calculated using the Pythagorean theorem applied to the frustum geometry (Equation 3):

$$g^2 = h^2 + [R2 - R1]^2 \quad (3)$$

The diameter, radius, and height (h) values of the specimens were measured prior to testing using a stereomicroscope (Discovery V20, Zeiss, Oberkochen, Germany) and a digital caliper (Starrett® 727, Starrett, Itu, Brazil).

After completion of the push-out test, the samples were analyzed under a Discovery V20 stereomicroscope (Discovery V20, Zeiss, Oberkochen, Germany) to determine the type of failure presented. The failures were classified as follows:

a) Adhesive: complete displacement of the post together with the resin cement;

b) Predominantly adhesive: failure present in the post and also at the dentin interface;

c) Cohesive in dentin: failure located within the dentin, where a portion of dentin is displaced;

d) Cohesive in post: failure located within the intraradicular post, where a portion of the post is displaced;

e) Mixed: simultaneous presence of adhesive and cohesive failures within the same sample.

Statistical analysis

Statistical analysis was performed using jamovi version 1.6 (The jamovi project, Sydney, Australia). Data normality was assessed using the Shapiro–Wilk test, and homogeneity of variances was evaluated with Levene's test. A two-way analysis of variance (ANOVA) was conducted to evaluate the effects of the factors "root third" (cervical, middle, and apical) and "group" (Fiber, Photo, and Fiber+Photo), as well as their interaction, on bond strength values. When statistically significant differences were detected, pairwise comparisons were performed using Tukey's post hoc test. The level of significance was set at $\alpha = 0.05$.

RESULTS

In the push-out test, mean bond strength (MPa) varied significantly among the root thirds,

with the highest values consistently observed in the cervical third and the lowest in the apical third across all experimental groups (Table 2). No significant differences were observed among activation systems within each root third.

Data were normally distributed according to the Shapiro–Wilk test ($p > 0.05$), and homogeneity of variances was confirmed by Levene's test ($p = 0.069$), satisfying the assumptions for parametric analysis.

Two-way ANOVA revealed a significant effect of root third ($p < 0.001$), confirming differences in bond strength among cervical, middle, and apical regions. No significant main effect of activation system was observed ($p = 0.117$). Although a significant interaction between factors was detected ($p < 0.001$), post hoc comparisons indicated no statistically significant differences among activation systems within each root third.

Stereomicroscopic analysis revealed different failure modes across groups and root thirds. Adhesive failures were the most frequent type, predominating in all experimental groups and root thirds, particularly in the Photo group at the cervical third (Figure 3A). Predominantly adhesive failures were also frequently observed across all conditions (Figure 3B).

Cohesive failures in dentin and in the post occurred less frequently but were present in all groups and root thirds (Figures 3C and 3D).

Table 2 - Mean bond strength (MPa) and standard deviation for each experimental group across root thirds, followed by Tukey's post hoc test ($p < 0.05$)

Third	Group	Mean ± SD (MPa)
C	Fiber+Photo	5.87 ± 0.982 ^{Aa}
	Photo	5.00 ± 0.904 ^{Aa}
	Fiber	3.88 ± 0.396 ^{Aa}
M	Fiber+Photo	4.19 ± 0.496 ^{Ba}
	Photo	4.19 ± 1.122 ^{Ba}
	Fiber	4.32 ± 0.779 ^{Ba}
A	Fiber+Photo	1.53 ± 0.965 ^{Ca}
	Photo	2.30 ± 1.167 ^{Ca}
	Fiber	2.07 ± 1.048 ^{Ca}

Legend: Different uppercase letters indicate statistically significant differences among root thirds. Lowercase letters indicate no significant differences among groups within the same third (Tukey test, $p < 0.05$).

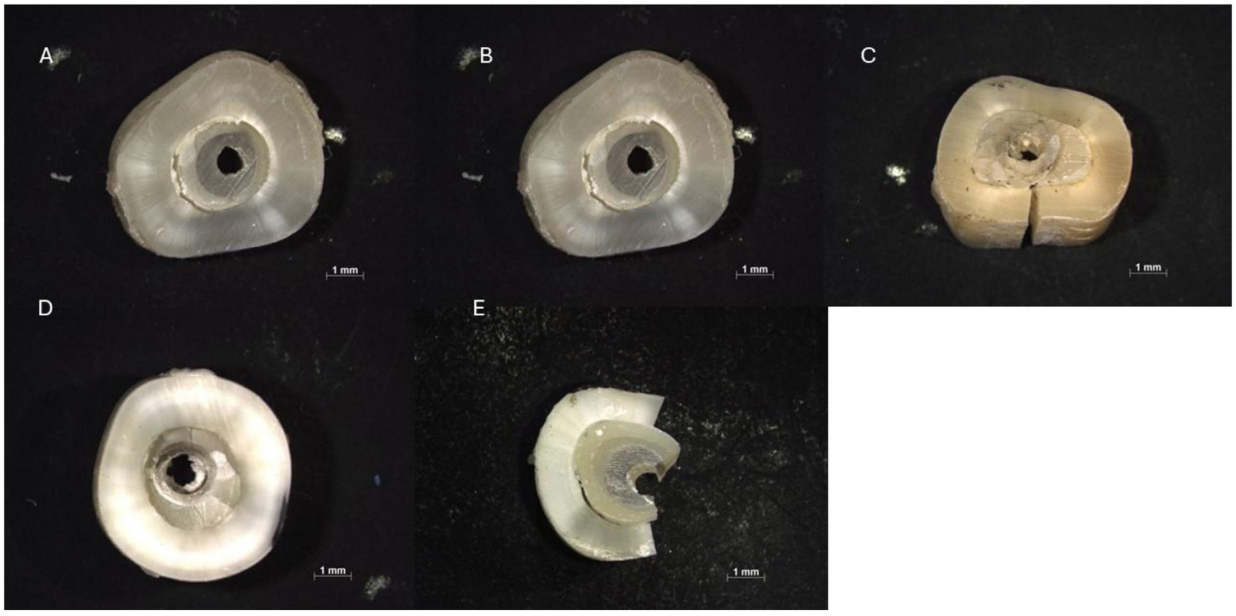


Figure 3 - Stereomicroscopic analysis of different types of failures. **Legend: A)** Adhesive failure; **B)** Predominantly adhesive failure; **C)** Cohesive failure in dentin; **D)** Cohesive failure in the post; **E)** Mixed failure.

Notably, the Photo group in the apical third exhibited predominantly cohesive failure in the post, whereas the Fiber group in the cervical third showed predominantly cohesive failure in dentin. Mixed failures were also observed among the evaluated groups, with a higher frequency in the Photo group at the apical third, which represented the most unfavorable failure pattern.

Mixed failures were also observed across all groups, with higher frequency in the Photo group at the apical third, which represented the most unfavorable failure pattern among the evaluated conditions (Figure 3E).

The Fiber+Photo (F+P) group, characterized by fiber optic photoactivation followed by supplemental conventional light curing, showed predominantly adhesive and predominantly adhesive failures across all root thirds, with a relatively homogeneous distribution pattern. Similarly, the Fiber (F) group, in which posts were photoactivated exclusively through the fiber optic system, demonstrated comparable behavior, with adhesive failures remaining the most frequent mode throughout the cervical, middle, and apical regions (Figure 4).

In contrast, the Photo (P) group (control), which received only conventional photoactivation without fiber optic assistance, exhibited a more variable failure pattern depending on root depth. In the cervical third, adhesive failures predominated, similar to the experimental groups. However, in the middle third, an increase in cohesive failures in dentin was observed, while the apical third showed a marked shift toward mixed failures, accompanied by a reduction in adhesive failures. In the apical third, the Photo (P) group showed a marked shift toward mixed failures, accompanied by a reduction in adhesive failures, representing the most unfavorable failure distribution among all groups. This change in failure pattern was more pronounced in the apical region compared to the cervical and middle thirds.

DISCUSSION

Several studies have been conducted aiming to optimize the degree of photopolymerization in restorative dentistry, considering its importance for adhesive strength and the clinical success of prosthetic rehabilitation. Inadequate polymerization among the adhesive system components can significantly compromise their mechanical properties and the longevity of the cementation [16,25-27]. In this context, the present study evaluated the effect of incorporating optical fiber into the photopolymerization of 3D-printed posts on the adhesive strength along the root thirds. This approach introduces a clinically relevant strategy to improve internal light delivery within customized 3D-printed post systems.

The 3D-printed post material, which accommodates the optical fiber insertion, was fabricated from a translucent resin. Due to its optical translucency, incident light penetrates beneath the surface and is scattered, emerging

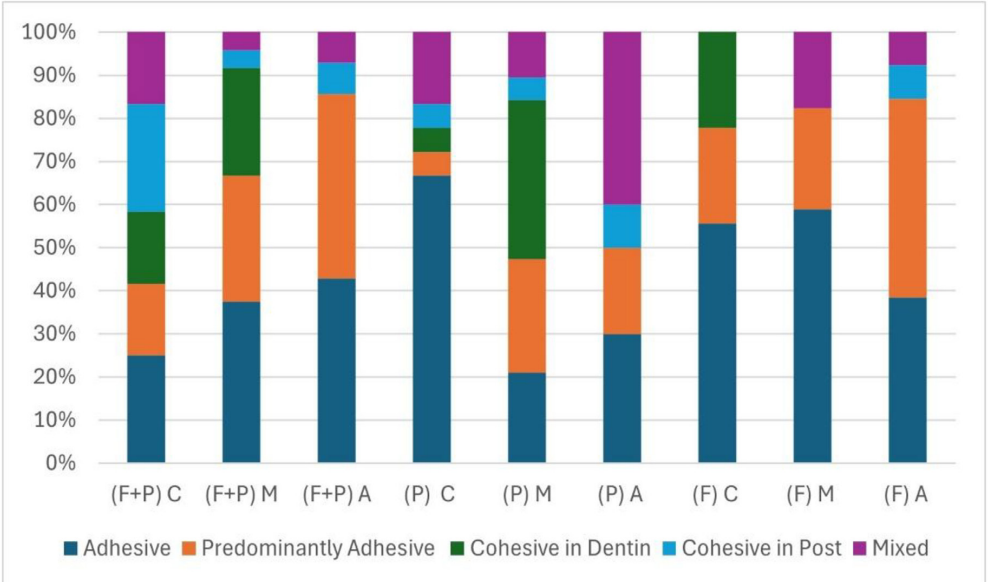


Figure 4 - Percentage distribution of failure modes observed in each experimental group across the cervical, middle, and apical root thirds.

at locations distinct from the point of incidence a phenomenon known as subsurface scattering, described by the bidirectional surface scattering reflectance distribution function (BSSRDF) [28]. This optical property facilitates efficient light transmission from the fiber optic core through the post material to the surrounding resin cement within the root canal. The delivery of light at an appropriate wavelength (405 nm) and sufficient irradiance enables more effective photoactivation of the adhesive system and resin cement, thereby promoting improved bond formation [29-32].

Bond strength was significantly influenced by root third ($p < 0.001$), with higher values observed in the cervical region and lower values in the apical region, regardless of the activation system evaluated. The highest mean bond strength was recorded in the FIBER+PHOTO group at the cervical third (5.87 MPa), whereas the lowest was observed in the FIBER group at the apical third (1.53 MPa). These findings are consistent with established principles of light-activated polymerization, which demonstrate that curing efficacy depends on light penetration depth and the optical properties of the intervening media. Light intensity attenuates with increasing distance from the source, and when the target depth exceeds the effective penetration range, inadequate polymerization occurs particularly in apical canal regions where light transmission is inherently limited [33-35].

Furthermore, a significant interaction was observed between activation system and root third ($p < 0.001$), suggesting that photoactivation effectiveness varies with canal depth. However, post hoc analysis within each root third individually revealed no statistically significant differences among activation systems ($p > 0.05$), indicating that fiber optic light delivery alone was insufficient to significantly alter bond strength at any specific level.

Several factors may explain this apparent paradox. First, the flowable composite resin layer used for post customization may have acted as an optical barrier, attenuating light transmission from the fiber optic core to the surrounding adhesive system and resin cement. The thickness and optical properties of this intermediate layer could have compromised light dissipation and reduced photoactivation efficiency. Second, the Bio Splint resin used for post fabrication, despite being translucent, may have exhibited optical scattering properties that diffused rather than efficiently transmitted the incident light. These findings contrast with those of Inagati et al. (2022), who reported significantly higher degrees of conversion when using fiber optic activation systems [36]. Notably, their study employed non-customized posts without an intermediate composite layer, enabling more direct and efficient light transmission from the fiber optic to the luting cement.

Resin cements have been widely adopted in prosthetic dentistry due to their favorable physical properties, including high tensile and compressive strength, low solubility, good fracture toughness, and availability in various shades that facilitate esthetic integration [37]. However, numerous clinical scenarios limit or prevent adequate light activation, directly compromising material performance. Insufficient irradiance results in reduced degree of conversion, which consequently impairs the mechanical properties, bond strength, and clinical longevity of resin cements [38-41].

This study aimed to enhance light delivery to the apical third through fiber optic technology. However, stereomicroscopic analysis revealed that adhesive failures predominated across all experimental groups and root thirds, with the highest frequency observed in the PHOTO group at the cervical third. This failure pattern suggests that, despite the proposed enhancement in photoactivation provided by the fiber optic system, the adhesive interface remains the most vulnerable component of the post-cement-dentin complex, even in regions with optimal light access.

The PHOTO control group, which received only conventional photoactivation without fiber optic assistance, exhibited greater variability in failure patterns among root thirds. Notably, cohesive failures in dentin predominated in the middle third, while mixed failures were most frequent in the apical third the region most compromised by light attenuation. This heterogeneous failure distribution highlights the reduced predictability and compromised polymerization efficacy of conventional photoactivation in deeper canal regions, attributable to exponential light attenuation and the complex three-dimensional anatomy of root canals that impedes direct light transmission.

Conversely, the fiber optic-assisted groups (FIBER and FIBER+PHOTO) exhibited more consistent failure patterns, with adhesive

and predominantly adhesive failures predominating uniformly across all root thirds. This homogeneity suggests more stable and uniform light distribution provided by the fiber optic delivery system, although this improved consistency was not reflected in statistically significant differences in bond strength values. These findings underscore the multifactorial nature of adhesive bonding in root canals and highlight the need for future investigations with rigorous control of confounding variables, including the thickness of the intermediate composite customization layer, the optical transmission properties of materials employed, and the precision of fiber optic positioning and adaptation within the canal space.

Another potentially critical factor is light penetration depth. Light intensity attenuates exponentially in materials with limited optical transmission or in regions with complex geometry, compromising the degree of conversion and, consequently, the mechanical properties and bond strength of resin cements [33]. In the present study, the flowable composite resin used for post customization likely functioned as an optical barrier, particularly affecting light transmission to the apical region where conventional photoactivation is already inherently compromised.

Achieving adequate bond strength after cementation requires that the resin cement receives sufficient irradiance and exposure duration to reach optimal polymerization, particularly in apical regions where light penetration is most limited. The literature demonstrates that polymerization efficacy is influenced by multiple interdependent factors, including material composition, irradiance, wavelength, exposure duration, distance from the light source, and filler particle characteristics, all of which collectively determine the degree of conversion [38,42-47].

Therefore, the efficacy of fiber optic systems depends not only on their presence, but also on their integration within the post cement dentin assembly. A key novelty of the present study lies in the evaluation of fiber optic light delivery within a clinically relevant 3D-printed post system incorporating an intermediate composite customization layer. In this context, this intermediate layer likely attenuated the potential benefits of fiber optic technology.

Future investigations using 3D-printed posts without intermediate composite layers, allowing direct energy transfer from the fiber optic core to the cement, may demonstrate greater improvements in bond strength, particularly in apical regions. Additionally, optimization of post optical properties, reduction of customization layer thickness, or use of highly translucent composites should be systematically explored to maximize the clinical applicability of fiber optic-assisted photoactivation systems.

CONCLUSION

Bond strength decreased significantly from cervical to apical root thirds regardless of photoactivation method. Although fiber optic-assisted photoactivation improved the uniformity of failure patterns across canal depths, it did not result in statistically superior bond strength values compared with conventional photoactivation.

The fiber optic system demonstrated potential for more consistent polymerization throughout root canals; however, the intermediate composite customization layer likely attenuated light transmission, limiting clinical benefits. Future investigations employing 3D-printed posts without intermediate composite layers are warranted to fully evaluate the potential of fiber optic-assisted photoactivation in intraradicular cementation.

Acknowledgements

We would like to thank Fapesp for granting the Scholarship (2022/07378-8) and the Photonita – Metrologia Óptica company for providing the optical fiber.

Data availability

Repositories. https://repositorio.unesp.br/entities/publication/304d70dd-c22a-45a2-a362-bad79a8bbadf

Author's Contributions

MFS: Methodology. JFGS: Methodology, Writing, Original Draft Preparation, Data Curation. CGF: Writing, Original Draft Preparation, Validation. LCLG: Supervision, Validation, Project Administration. TJAPJ: Resources, Validation,

Project Administration, Supervision, Writing, Review and Editing.

Conflict of Interest

The authors have no conflicts of interest to declare.

Funding

Fapesp for granting the Scholarship (2022/07378-8)

Regulatory Statement

This study was conducted in accordance with all provisions of the local supervisory committee guidelines and policies, where it was waived due to the use of bovine teeth.

References

1. Costa Fartes OA, Resende LM, Cilli R, Carmo AMR, Baroudi K, Cortelli JR. Retention of provisional intraradicular retainers using fiberglass pins. J Int Soc Prev Community Dent. 2020;10(5):666-73. https://doi.org/10.4103/jispcd.JISPCD_298_20. PMid:33282778.
2. Goracci C, Ferrari M. Current perspectives on post systems: a literature review. Aust Dent J. 2011;56(Suppl. 1):77-83. https://doi.org/10.1111/j.1834-7819.2010.01298.x. PMid:21564118.
3. Maluly-Proni AT, Queiroz ME, Gomes MH, Suzuki TYU, Reis BDO, Santos PHD. Relined fiberglass posts: influence of resin opacity on the bond strength to intraradicular dentin. Braz Dent J. 2024;35:5746. https://doi.org/10.1590/0103-6440202405746. PMid:39045986.
4. Lee Y, Kim J, Shin Y. Push-out bond strength evaluation of fiber-reinforced composite resin post cemented with self-adhesive resin cement using different adhesive bonding systems. Materials (Basel). 2021;14(13):3639. https://doi.org/10.3390/ma14133639. PMid:34209908.
5. Balkenhol M, Wöstmann B, Rein C, Ferger P. Survival time of cast post and cores: a 10-year retrospective study. J Dent. 2007;35(1):50-8. https://doi.org/10.1016/j.jdent.2006.04.004. PMid:16750593.
6. Gutiérrez MA, Guerrero CA, Baldion PA. Efficacy of CAD/CAM glass fiber posts for the restoration of endodontically treated teeth. Int J Biomater. 2022;2022:8621835. https://doi.org/10.1155/2022/8621835. PMid:35096068.
7. Assis HC, Cronenbold TJ, Prado HS, Eyüboğlu TF, Özcan M, Sousa-Neto MD, et al. Role of post design and cement type in fiber post adaptation and retention. BMC Oral Health. 2026;26(1):320. https://doi.org/10.1186/s12903-025-07539-1. PMid:41566294.
8. Haralur SB, Alasmari TA, Alasmari MH, Hakami HM. Light transmission of various aesthetic posts at different depths and its effect on push-out bond strength, microhardness of luting cement. Medicina (Kaunas). 2022;58(1):75. https://doi.org/10.3390/medicina58010075. PMid:35056383.
9. Vieira C, Bachmann L, De Andrade Lima Chaves C, Correa Silva-Sousa YT, Correa Da Silva SR, Alfredo E. Light transmission and bond strength of glass fiber posts submitted to different surface treatments. J Prosthet Dent. 2021;125(4):674.e1-7. https://doi.org/10.1016/j.prosdent.2020.11.031. PMid:33431176.
10. Alves Morgan LFDS, Pinotti MB, Ferreira FM, Gomes GM, Silva GC, Albuquerque RDC, et al. Influence of light transmission through fiber posts: quantitative analysis, microhardness, and on bond strength of a resin cement. Indian J Dent Res. 2018;29(1):74-80. https://doi.org/10.4103/ijdr.IJDR_792_16. PMid:29442091.
11. Angnanon W, Thammajaruk P, Guazzato M. Effective luting agents for glass-fiber posts: a network meta-analysis. Dent Mater. 2023;39(12):1180-9. https://doi.org/10.1016/j.dental.2023.10.015. PMid:37845166.
12. Caughman WF, Chan DCN, Rueggeberg FA. Curing potential of dual-polymerizable resin cements in simulated clinical situations. J Prosthet Dent. 2001;85(5):479-84. https://doi.org/10.1067/mpr.2001.114842. PMid:11357075.
13. Taneja S, Kumari M, Gupta A. Evaluation of light transmission through different esthetic posts and its influence on the degree of polymerization of a dual cure resin cement. J Conserv Dent. 2013;16(1):32-5. https://doi.org/10.4103/0972-0707.105295. PMid:23349573.
14. Oliveira DCRS, Rocha MG, Souza-Júnior EJ, Rocha-Maia R, Puppin-Rontani RM, Sinhoreti MAC. The effect of shade and curing mode on cure efficiency of dual-cure resin cements. Braz Dent Sci. 2016;19(3):59-64. https://doi.org/10.14295/bds.2016.v19i3.1265.
15. Gonçalves JM, Sales TAM, Figueiredo CS, Mendonça RP, Silva Júnior JP, Silva TM, et al. Multi-peak light sources can improve the physical and mechanical properties of a zirconia- and diatomite-based dental resin: an in vitro study. Braz Dent Sci. 2025;28(2):e4750. https://doi.org/10.4322/bds.2025.e4750.
16. Ortiz-Magdaleno M, Bogarin-Topete ER, Cerda-Cristerna BI, Gutiérrez-Sánchez M. Effect of degree of conversion on the surface properties of polymerized resin cements used for luting glass fiber posts. J Prosthet Dent. 2023;130(2):256.e1-12. https://doi.org/10.1016/j.prosdent.2023.05.009. PMid:37357085.
17. Murata K, Miura H, Ikeda H, Yoshii S, Washio A, Kitamura C. Influence of Light Irradiation Modes on the Polymerization of Light-curing Resins in a Root Canal Model. Operative Dentistry. Endodontology and Periodontology. 2022;2(1):25-32.
18. Ferracane JL. Correlation between hardness and degree of conversion during the setting reaction of unfilled dental restorative resins. Dent Mater. 1985;1(1):11-4. https://doi.org/10.1016/S0109-5641(85)80058-0. PMid:3160625.
19. Silami FDJ, Tonani R, Alandia-Román CC, Pires-De-Souza FCP. Influence of different types of resin luting agents on color stability of ceramic laminate veneers subjected to accelerated artificial aging. Braz Dent J. 2016;27(1):95-100. https://doi.org/10.1590/0103-6440201600348. PMid:27007354.
20. Goracci C, Grandini S, Bossù M, Bertelli E, Ferrari M. Laboratory assessment of the retentive potential of adhesive posts: A review. J Dent. 2007;35(11):827-35. https://doi.org/10.1016/j.jdent.2007.07.009. PMid:17766026.
21. Magão PH, Santos AF, Chiok Ocaña LR, Rizzante FAP, Furuse AY. Water sorption and color stability of dental composites light-cured with a broadband LED device and different radiant exposures. Braz Dent Sci. 2024;27(3):e4379. https://doi.org/10.4322/bds.2024.e4379.
22. Meleka NM, El-Banna A, El-Korashy DI. Color stability and degree of conversion of amine-free dual cured resin cement used with two different translucencies of lithium disilicate ceramics. Braz Dent Sci. 2023;26(2):e3614. https://doi.org/10.4322/bds.2023.e3614.

23. Trenfield SJ, Awad A, Madla CM, Hatton GB, Firth J, Goyanes A, et al. Shaping the future: recent advances of 3D printing in drug delivery and healthcare. Expert Opin Drug Deliv. 2019;16(10):1081-94. https://doi.org/10.1080/17425247.2019.1660318. PMid:31478752.

24. Kouhi M, de Souza Araújo IJ, Asa'ad F, Zeenat L, Bojedla SSR, Pati F, et al. Recent advances in additive manufacturing of patient-specific devices for dental and maxillofacial rehabilitation. Dent Mater. 2024;40(4):700-15. https://doi.org/10.1016/j.dental.2024.02.006. PMid:38401992.

25. Alsayed B, Suliman AA, Clark W, Cook R, Sulaiman TA. Effect of photo-polymerization delay on the bond strength and microhardness of dual-polymerizing resin cements. Oper Dent. 2023;48(4):457-63. https://doi.org/10.2341/22-119-L. PMid:37352457.

26. Bhandari SS, Margasahayam SV, Shenoy VU, Patil AB, Surwade MA. Evaluation of the degree of conversion of flowable bulk fill and dual-cure composite resins for intracanal root reinforcement in teeth with structurally weakened roots: an in vitro Fourier transformer infrared study. J Conserv Dent Endod. 2025;28(12):1279-84. https://doi.org/10.4103/JCDE.JCDE_887_25. PMid:41438443.

27. Fidalgo-Pereira R, Torres O, Carvalho Ó, Silva FS, Catarino SO, Özcan M, et al. A scoping review on the polymerization of resin-matrix cements used in restorative dentistry. Materials (Basel). 2023;16(4):1560. https://doi.org/10.3390/ma16041560. PMid:36837188.

28. Nicodemus FE, Richmond JC, Hsia JJ, Ginsberg IW, Limperis T. Geometrical Considerations and Nomenclature for Reflectance. Washington, DC: National Bureau of Standards; 1977. https://doi.org/10.6028/NBS.MONO.160.

29. Ozturk N, Aykent F. Dentin bond strengths of two ceramic inlay systems after cementation with three different techniques and one bonding system. J Prosthet Dent. 2003;89(3):275-81. https://doi.org/10.1067/mpr.2003.37. PMid:12644803.

30. Han SH, Shimada Y, Sadr A, Tabata T, Nakagawa H, Sato T, et al. Effect of attenuated light through translucent zirconia on the interfacial adaptation and polymerization of resin cements. J Adhes Dent. 2023;25:219-30. https://doi.org/10.3290/J.JAD.B4586857. PMid:37910068.

31. Pekkan G, Hekimoglu C. Evaluation of shear and tensile bond strength between dentin and ceramics using dual-polymerizing resin cements. J Prosthet Dent. 2009;102(4):242-52. https://doi.org/10.1016/S0022-3913(09)60163-3. PMid:19782827.

32. Silva TM, Faria Petrucelli N, Mendonça RP, Silva JP Jr, Campos TMB, Paiva Gonçalves SE. Impact of photoinitiator quality on chemical-mechanical properties of dental adhesives under different light intensities. Braz Dent Sci. 2023;26(1):e3704. https://doi.org/10.4322/bds.2023.e3704.

33. You S, Wang P, Schimelman J, Hwang HH, Chen S. High-fidelity 3D printing using flashing photopolymerization. Addit Manuf. 2019;30:100834. https://doi.org/10.1016/j.addma.2019.100834. PMid:32832382.

34. Layani M, Wang X, Magdassi S. Novel materials for 3D printing by photopolymerization. Adv Mater. 2018;30(41):e1706344. https://doi.org/10.1002/adma.201706344. PMid:29756242.

35. Shin S, Kwon Y, Hwang C, Jeon W, Yu Y, Paik HJ, et al. Visible-light-driven rapid 3D printing of photoresponsive resins for optically clear multifunctional 3D objects. Adv Mater. 2024;36(19):e2311917. https://doi.org/10.1002/adma.202311917. PMid:38288894.

36. Inagati CM, Grangeiro MTV, Rossi NR, Tribst JPM, Nakano LJN, de Carvalho PCK, et al. Effect of light emission through an optical fiber device on the bond strength of a hollow experimental intraradicular post. J Adhes Dent. 2022;24(1):325-33. https://doi.org/10.3290/J.JAD.B3240659. PMid:35980241.

37. Christensen GJ. The rise of resin for cementing restorations. J Am Dent Assoc. 1993;124(10):104-5. https://doi.org/10.14219/jada.archive.1993.0201. PMid:8408999.

38. Rueggeberg FA, Craig RG. Correlation of parameters used to estimate monomer conversion in a light-cured composite. J Dent Res. 1988;67(6):932-7. https://doi.org/10.1177/00220345880670060801. PMid:3170905.

39. Yu C, Schimelman J, Wang P, Miller KL, Ma X, You S, et al. Photopolymerizable biomaterials and light-based 3D printing strategies for biomedical applications. Chem Rev. 2020;120(19):10695-743. https://doi.org/10.1021/acs.chemrev.9b00810. PMid:32323975.

40. Ramos MB, Pegoraro TA, Pegoraro LF, Carvalho RM. Effects of curing protocol and storage time on the micro-hardness of resin cements used to lute fiber-reinforced resin posts. J Appl Oral Sci. 2012;20(5):556-62. https://doi.org/10.1590/S1678-77572012000500011. PMid:23138743.

41. De J, Filho M. Dental zirconia generations: a comparative study of translucency parameters and light transmittance across varying thicknesses. Braz Dent Sci. 2024;27(3):4021. https://doi.org/10.4322/bds.2024.e4021.

42. Koupis NS, Vercruysse CWJ, Marks LAM, Martens LC, Verbeeck RMH. Curing depth of (polyacid-modified) composite resins determined by scraping and a penetrometer. Dent Mater. 2004;20(10):908-14. https://doi.org/10.1016/j.dental.2004.01.001. PMid:15501318.

43. Ferracane JL, Greener EH. The effect of resin formulation on the degree of conversion and mechanical properties of dental restorative resins. J Biomed Mater Res. 1986;20(1):121-31. https://doi.org/10.1002/jbm.820200111. PMid:3949822.

44. Asmussen E, Peutzfeldt A. Influence of UEDMA, BisGMA and TEGDMA on selected mechanical properties of experimental resin composites. Dent Mater. 1998;14(1):51-6. https://doi.org/10.1016/S0109-5641(98)00009-8. PMid:9972151.

45. David-Pérez M, Ramírez-Suárez JP, Latorre-Correa F, Agudelo-Suárez AA. Degree of conversion of resin-cements (light-cured/dual-cured) under different thicknesses of vitreous ceramics: systematic review. J Prosthodont Res. 2022;66(3):385-94. https://doi.org/10.2186/jpr.JPR_D_20_00090. PMid:34853236.

46. Santos M, Fidalgo-Pereira R, Torres O, Carvalho O, Henriques B, Özcan M, et al. The impact of inorganic fillers, organic content, and polymerization mode on the degree of conversion of monomers in resin-matrix cements for restorative dentistry: a scoping review. Clin Oral Investig. 2024;28(8):454. https://doi.org/10.1007/s00784-024-05829-6. PMid:39066793.

47. Martins FV, Vasques WF, Fonseca EM. How the variations of the thickness in ceramic restorations of lithium disilicate and the use of different photopolymerizers influence the degree of conversion of the resin cements: a systematic review and meta-analysis. J Prosthodont. 2019;28(1):e395-403. https://doi.org/10.1111/jopr.12920. PMid:29882387.

Juliana de Freitas Gouveia Silva
(Corresponding address)
Universidade Estadual de São Paulo, Instituto de Ciência e Tecnologia, Departamento de Materiais Dentários e Prótese Dentária. São José dos Campos, SP, Brazil.
Email: juliana.gouveia@unesp.br

Editor-in-chief: Sergio Eduardo de Paiva Gonçalves
Editor: João Paulo Mendes Tribst

Date submitted: 2026 Mar 26
Accept submission: 2026 Jun 19